

Article

Development of a Temperature-Responsive Polymer Network with Enhanced Transparency and Volume Shrinkage via Star-Shaped PEG-b-PNIPA Block Copolymer

Kai Kawabata¹, Taiki Hoshino^{2,3,4}, and Yukikazu Takeoka^{1,*}

¹ Department of Molecular & Macromolecular Chemistry, Nagoya University, Nagoya 464-8603, Japan

² International Center for Synchrotron Radiation Innovation Smart, Tohoku University, 468-1 Aramaki-Aza-Aoba, Aoba-ku, Sendai 980-8572, Japan

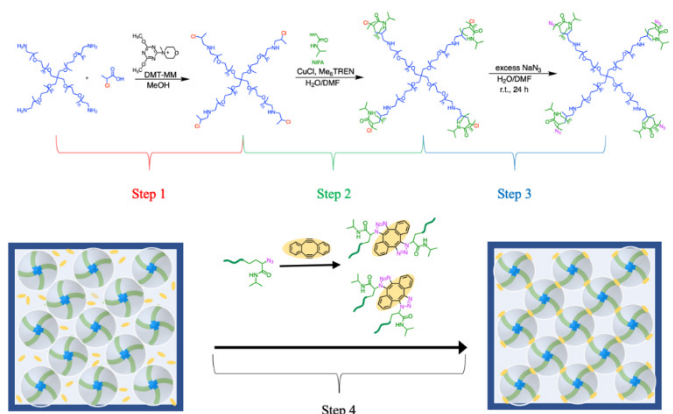
³ RIKEN SPring-8 Center, 1-1-1 Kouto, Sayo-cho 679-5148, Japan

⁴ Institute of Multidisciplinary Research for Advanced Materials, Tohoku University, 2-1-1 Katahira, Aoba-ku, Sendai 980-8577, Japan

* Correspondence: ytakeoka1@mac.com

Received: 21 March 2025; Revised: 4 June 2025; Accepted: 1 July 2025; Published: 10 July 2025

Abstract: In this study, a temperature-responsive polymer network was successfully synthesized by using a 4-arm star-shaped polyethylene glycol (PEG) derivative as an initiator and polymerizing *N*-isopropylacrylamide (NIPA) as a secondary acrylamide. The resulting star-shaped block copolymer was used as a building block to prepare a polymer network. Detailed analysis of the polymerization process (including SEC and ¹H NMR) confirmed the successful synthesis and high control over the star-shaped block copolymer structure. The obtained star-shaped block copolymer was crosslinked under semi-dilute conditions via a click reaction, in which the hydrophilic PEG was incorporated in an ordered manner into the poly(*N*-isopropylacrylamide) (PNIPA) network. This network exhibits a lower critical solution temperature (LCST) behavior at 32.5 °C in water. The introduction of PEG led to unique properties, such as volume shrinkage upon heating while maintaining optical transparency, due to the effective suppression of phase separation within the network. This advancement overcomes the limitations of conventional PNIPA-based gels and expands their potential applications in optical sensors, actuators, and biomedical devices. The results highlight the promising applications of this polymer network in the development of advanced smart materials.



Keywords: temperature-responsive polymer gel; LCST; star-shaped block copolymer; click chemistry; optical transparency

1. Introduction

Polymer systems that exhibit a sharp change in solubility due to significant alterations in their interaction with solvents upon temperature changes have been extensively studied. In systems where the polymer does not dissolve at low temperatures but dissolves at high temperatures, the upper critical solution temperature (UCST) is observed [1,2], which intuitively correlates with the temperature-dependent solubility changes of typical substances. On the other hand, there are also systems that dissolve well at low temperatures but fail to dissolve at higher temperatures, which are classified as polymers exhibiting the lower critical solution temperature (LCST) [3,4]. Such systems are often observed in structure-forming solvents like water or ionic liquids [5].



Copyright: © 2025 by the authors. This is an open access article under the terms and conditions of the Creative Commons Attribution (CC BY) license (<https://creativecommons.org/licenses/by/4.0/>).

Publisher's Note: Scilight stays neutral with regard to jurisdictional claims in published maps and institutional affiliations.

Among polymers that exhibit LCST behavior in water, poly(*N*-isopropylacrylamide) (PNIPA), which consists of *N*-isopropylacrylamide (NIPA), has been the most studied [6]. PNIPA shows an LCST of about 32 °C in water, and its crosslinked gel, which consists of polymer chains forming a network, exhibits reversible swelling at low temperatures and contraction at high temperatures due to temperature-dependent interactions in water. This temperature responsiveness has led to extensive research into the application of PNIPA gels in sensors [7], catalysts [8], drug delivery systems [9], and actuators [10,11]. Although certain applications have shown promise, issues such as the slow rate of volume change of the gel remain a challenge, preventing widespread commercialization. Specifically, the very slow contraction rate and optical turbidity of the gel due to network phase separation prior to contraction can pose practical problems [12]. Polymer gels that undergo large volumetric changes in response to environmental stimuli can transiently enter thermodynamically unstable states under certain conditions. In such cases, the polymer chains within the network may phase-separate into aggregated and expanded domains (Figure 1). This results in the formation of refractive index fluctuations on the scale of visible wavelengths within the polymer network, leading to strong light scattering and macroscopic turbidity. Moreover, returning from the unstable state to the thermodynamically stable state can take a considerable amount of time, significantly slowing the gel's response. Such turbidity and delayed responsiveness can impair the performance or functionality of devices such as optical sensors, actuators, and biomedical systems. Therefore, it is essential to develop strategies for material design or structural control that can suppress or prevent these undesirable phenomena. To improve the contraction rate, methods such as introducing pores into the gel [13] or incorporating dangling chains that are not crosslinked at one end [14,15] have been explored. However, these methods still face the challenge of the gel losing optical transparency due to network phase separation during contraction. Therefore, if a gel can be obtained that contracts rapidly while maintaining optical transparency, it would have great potential for applications in optical sensors and other devices.

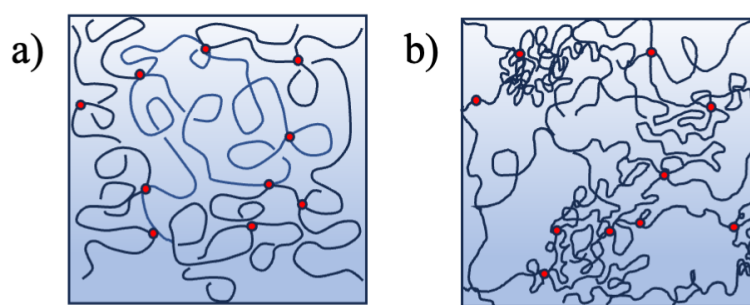


Figure 1. Conceptual diagrams showing the difference in the network structure of NIPA gel obtained from conventional free-radical polymerization, which is (a) fully swollen at low temperatures in water and (b) phase separated near the transition temperature: It segregates along regions with sparse and dense network densities, and the difference in refractive indices between these regions scatters visible light, making it appear white.

We have previously synthesized block copolymers by combining temperature-responsive PNIPA obtained through living polymerization with polymers that dissolve in water over a wide temperature range, and have explored a method of obtaining polymer networks by crosslinking their ends under appropriate conditions [16,17]. For example, after synthesizing a 4-arm star-shaped PNIPA, *N,N*-dimethylacrylamide (DMA), which dissolves in water over a wide temperature range, was polymerized, and the star-shaped block copolymer was crosslinked under appropriate conditions to successfully form a polymer network [18,19]. In this system, excess amounts of the crosslinking agent methylene bis-acrylamide (BIS), commonly used for gel preparation, were employed for crosslinking the star-shaped block copolymers, resulting in the formation of particles derived from BIS between the star-shaped block copolymers, as revealed by small-angle X-ray scattering (SAXS). The influence of these BIS-derived particles on the gel's properties is currently being investigated, but to accurately understand the behavior as the polymer network with an ordered structure made from the block copolymers mentioned above, it is desirable to prepare a system without the presence of BIS-derived particles. Furthermore, in order to achieve a high degree of functionality in polymer chain end-group transformations using halogenated alkyl groups, it is necessary to stabilize the halogenated chain ends during polymerization. In block copolymerization using acrylamide derivatives, it is known that the disappearance of halogenated terminal groups is significantly greater for tertiary acrylamides than for secondary acrylamides. This is due to the increase in electron density of the amide group, which results in increased alkyl substitution on the nitrogen atom, promoting the cyclization reaction of the halogenated terminal groups and leading to faster termination and the disappearance of active polymer chains. Unfortunately, polymerization using copper complexes makes it difficult to effectively activate these unstable

species, inhibiting the transformation or substitution reactions of the halogenated terminal groups. This complexity makes polymerization control difficult and hinders the desired terminal group modification. Therefore, when synthesizing block copolymers, it is preferable to choose secondary acrylamide derivatives like NIPA, as reactive halogenated alkyl groups will remain at the polymer chain ends, allowing for subsequent modification and the introduction of new polymer structures [20].

If structural challenges and synthetic inconveniences of the polymer network can be avoided, it will be possible to prepare polymer networks with a more ideally ordered structure. In this study, we used a derivative of a tetrafunctional star-shaped polymer made from polyethylene glycol (PEG), which exhibits hydrophilicity over a wide temperature range, as the initiator, and polymerized NIPA as a secondary acrylamide to synthesize a star-shaped block copolymer. Furthermore, under appropriate network formation conditions, we coupled the ends of this star-shaped block copolymer through a click reaction, introducing hydrophilic PEG into the structure of the PNIPA exhibiting LCST in an ordered manner. As a result, the obtained gel was shown to maintain optical transparency while undergoing volume reduction upon an increase in temperature.

2. Experimental Part

2.1. Materials

The 4-arm star-shaped polymer consisting of polyethylene glycol (PEG) chains, with amino groups at the ends and an average molecular weight of 2000 (4-ArmPEG-Amine), was purchased from Funakoshi (Manufacturer: Biopharma PEG Scientific, Watertown, MA, USA). 2-Chloropropionic Acid, 4-(4,6-Dimethoxy-1,3,5-triazin-2-yl)-4-methylmorpholinium Chloride (DMT-MM), Lithium bromide (LiBr), 5,6,11,12-Tetradehydrodibenzo[a,e]cyclooctene (DIBOD), and dibenzocyclooctyne-amine (DBCO-Amine) were purchased from Tokyo Chemical Industry Co., Ltd., Tokyo, Japan. Methanol (MeOH), chloroform, *N,N*-dimethylformamide (DMF), tetrahydrofuran (THF), acetonitrile, hydrochloric acid (HCl), copper(I) chloride (CuCl), and sodium azide (NaN₃) were purchased from Kishida Chemical Co., Ltd., Osaka, Japan. DMF used as a synthetic solvent was purified by vacuum distillation. CuCl was dissolved in concentrated hydrochloric acid, and the resulting solution was dropped into water. The precipitate was purified by suction filtration and drying. *N*-isopropylacrylamide (NIPA) was obtained from KJ Chemicals, Tokyo, Japan and tris(2-dimethylaminoethyl)amine (Me₆TREN) was provided by Mitsubishi Chemical, Tokyo, Japan. Both were purified by recrystallization and vacuum distillation. Ultrapure water was obtained by purifying tap water using a Direct-Q system (Merck) (resistivity 18.2 MΩ·cm). Ion-exchange water was obtained using a G-5C cartridge-type water purifier purchased from Organo, Chiba, Japan. Pentaerythritoltetra(2-chloropropionate) (PETCP) was synthesized on request by Tokyo Chemical Industry Co., Ltd., Tokyo, Japan.

2.2. Synthesis of Initiator from 4-ArmPEG-Amine

An amide condensation reaction using DMT-MM was employed to synthesize a 4-arm initiator containing PEG chains. 0.48 g of 4-ArmPEG-Amine, 145 μL of 2-Chloropropionic Acid, 0.93 g of DMT-MM, and 90 mL of MeOH were added to a 300 mL round-bottom flask, which was wrapped with aluminum foil to shield it from light. The synthetic scheme is shown in Figure 2, Step 1. The mixture was stirred at room temperature for 24 h. After stirring, the solvent was removed using a rotary evaporator. The crude product was purified by silica gel column chromatography (CHCl₃/MeOH = 2:3), yielding a viscous liquid (192.5 mg, 41% yield). The resulting sample was dissolved in CDCl₃ and analyzed by ¹H NMR.

2.3. Synthesis of End-Cl 4-Arm PEG-b-PNIPA

The 4-arm initiator containing PEG chains obtained in Section 2.2 was used to synthesize end-Cl 4-arm star-shaped PEG-b-PNIPA by living radical polymerization of NIPA. First, 1.84 g of NIPA and 192.5 mg of the 4-arm initiator were placed in a 200 mL round-bottom flask, and 5.61 mL of DMF was added under a nitrogen atmosphere in a glove box. The flask was sealed with a septum, removed from the glove box, and 3.44 mL of ultra-pure water, previously purged with nitrogen, was added using a syringe. Next, nitrogen bubbling was performed for more than 30 min at room temperature to prepare the monomer solution. Then, 29.3 mg of CuCl was placed in a 100 mL round-bottom flask, and 79.2 μL of Me₆TREN was added under nitrogen in a glove box. The solution was immersed in an ice water bath (4 °C) and stirred for 1 h to decompose the copper catalyst. The prepared monomer solution was then added via syringe (10.29 mL) under nitrogen flow, and the reaction was stirred at 4 °C for 120 min. The final monomer concentration in the reaction solution was 1.2 mol L⁻¹, and the volume ratio of DMF to water was 1:1, with a molar ratio of CuCl:Me₆TREN:NIPA:initiator = 4:4:200:1. The synthetic scheme is shown

in Figure 2, Step 2. During the polymerization, a small sample of the reaction solution was withdrawn using a syringe, and the polymerization was stopped by continuously blowing air for approximately 1 min. The sample was analyzed by ^1H NMR and SEC to monitor the progress of the reaction. The sample was dissolved in acetone- d_6 for ^1H NMR analysis. The remaining polymerization solution was diluted with THF and purified using a silica gel column to remove the copper catalyst. After catalyst removal, the solution was concentrated using a rotary evaporator. Dialysis was performed using a Spectra/Por6[®] Dialysis Membrane (MWCO: 1000) for 2 days in methanol, followed by 3 days in ion-exchange water. After dialysis, the product was lyophilized using a freeze dryer (FDU-1200, TOKYO RIKAKIKAI CO., LTD., Tokyo, Japan) to obtain a white solid. The final sample was dissolved in SEC elution solvent, filtered through a Millex-LCR 13 mm membrane filter (pore size 0.45 μm), and analyzed by SEC. The sample was also dissolved in acetone- d_6 for ^1H NMR analysis.

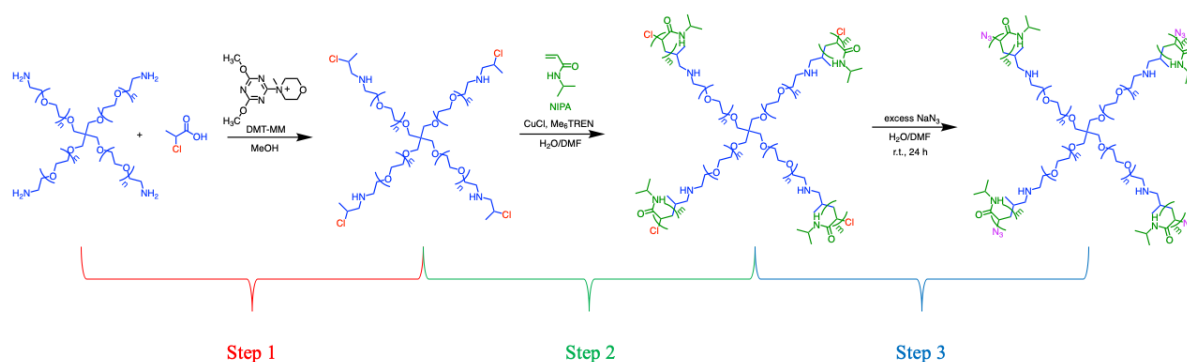


Figure 2. Synthesis of 4-ArmPEG-PNIPA with azide group at the end, Step 1: Synthesis of 4-arm initiator containing PEG, Step 2: Synthesis of end-Cl 4-arm star-shaped PEG-b-PNIPA, Step 1: Terminal azidation of tetrabranch PEG-b-PNIPA.

2.4. Synthesis of End- N_3 4-Arm Star-Shaped PEG-b-PNIPA

Referring to previously reported procedures, a 4-arm star-shaped PEG-b-PNIPA with an azide group at the end was synthesized [16–18]. The polymerization of NIPAA was carried out using the same method as in 2.3, and after 80 min, 0.29 g of NaN_3 dissolved in 1.55 mL of ultrapure water was added to the reaction solution (1.03 mL). The mixture was stirred at room temperature for 24 h. The synthetic scheme is shown in Figure 2, Step 3. The reaction solution was diluted with THF, and the copper catalyst was removed by silica gel column chromatography. Dialysis was performed using a Spectra/Por 6[®] Dialysis Membrane (MWCO: 1000) for 2 days in methanol, followed by 3 days in ion-exchange water. After dialysis, the product was lyophilized to obtain a white solid. The final sample was analyzed by ^1H NMR (acetone- d_6) and infrared spectroscopy.

2.5. Azidation Reaction Efficiency of End- N_3 4-Arm Star-Shaped PEG-b-PNIPA

The azide content of the end- N_3 4-arm star-shaped PEG-b-PNIPA synthesized in 2.4 was quantified. 97.5 mg (5.0×10^{-3} mmol) of the end- N_3 4-arm star-shaped PEG-b-PNIPA was placed in a 10 mL round-bottom flask with a magnetic stirrer. Anhydrous acetonitrile (1.5 mL) and 3.6 mg of DBCO-amine were added in a nitrogen atmosphere and stirred at room temperature for 24 h. Dialysis was performed using a Spectra/Por 6[®] Dialysis Membrane (MWCO: 1000) for 1 day in methanol, followed by 2 days in ion-exchange water. After dialysis, the product was lyophilized to obtain a white solid. The final sample was analyzed by ^1H NMR (acetone- d_6) and infrared spectroscopy.

2.6. Synthesis of End- N_3 4-Arm Star-Shaped PNIPA

For comparison, end- N_3 4-arm star-shaped PNIPA was synthesized from PNIPA only, following a previously reported procedure [17]. PETCP was used as the initiator for the 4-arm structure.

2.7. Preparation of PEG-b-PNIPA Gel via End-to-End Huisgen Cycloaddition of End- N_3 4-Arm Star-Shaped PEG-b-PNIPA

To prepare a gel from end- N_3 4-arm star-shaped PEG-b-PNIPA, the conditions for achieving a semi-dilute state of the polymer in a good solvent were investigated by dynamic light scattering (DLS) measurements (described later). End- N_3 4-arm star-shaped PEG-b-PNIPA was dissolved in acetonitrile to prepare solutions with

volume fractions $\Phi = 0.08, 0.12$, and 0.16 . The mixture was treated with ultrasonic waves for 30 min and allowed to stand overnight. DIBOD, in a stoichiometric amount (2 equivalents to end- N_3 4-arm star-shaped PEG-b-PNIPA), was then added, and the mixture was stirred for about 1 min until fully dissolved. It was then left at room temperature for at least 3 days to form the gel. A similar method was used to prepare the PNIPA gel from end- N_3 4-arm star-shaped PNIPA.

2.8. Proton Nuclear Magnetic Resonance (1H NMR) Measurement

Measurements were performed using a 400 MHz NMR (JEOL, Akishima City, Japan). Acetone- d_6 (Kanto Chemical, Tokyo, Japan) and chloroform- d_1 (Kanto Chemical), each containing 0.03% (v/v) TMS as the internal standard, were used as solvents. The number of scans was set to 16.

2.9. Size Exclusion Chromatography (SEC) Measurement

2.9.1. For PEG-b-PNIPA Systems

SEC measurements were performed using an ultraviolet detector (UV-41, Shodex, Kyoto, Japan) and a differential refractive index detector (RI-101, Shodex, Kyoto, Japan). The columns used were DS-4 (Shodex) and THF solvent columns KF-803L and KF-804L (Shodex) connected in sequence. The UV detector was set to a measurement wavelength of 254 nm. Molecular weight and molecular weight distribution were calculated from the calibration curve prepared using polystyrene standards.

2.9.2. For PNIPA Systems

The measurements were conducted using a SHIMADZU LC-20AD pump, SIL-20AHT autosampler, RID-10A differential refractive index detector, and CTO-20A temperature controller. The columns used were Shodex KW-G 6B (guard column), KW-804 (two columns), and KW-802.5 (two columns) connected in sequence. LiBr was dissolved in DMF at a concentration of 5 mmol L^{-1} and stirred overnight, and the resulting solution was used as the eluent. The system was stabilized for approximately 3 h under the measurement conditions, with a flow rate of 1.0 mL/min and an oven temperature of 40 °C. The molecular weight and molecular weight distribution were calculated based on a calibration curve created from measurements of polymethyl methacrylate standards.

2.10. Infrared Absorption Spectroscopy (IR) Measurement

The measurements were conducted using a Fourier-transform infrared spectrometer, NICOLET iS50 (Thermo Scientific, Waltham, MA, USA). The scan was performed 32 times with a data interval of 0.482 cm^{-1} , and the analysis was done using OMNIC software (Spectra Version 2.2). The measurements were carried out using the KBr pellet method, where approximately 1 mg of the sample and 100 mg of KBr were finely ground in an agate mortar, placed in a pellet mold, and pressed using a small hydraulic press (Specac, Orpington, UK).

2.11. UV-Vis Transmittance Measurement

End-Cl 4-arm star-shaped PNIPA and end-Cl, N_3 4-arm star-shaped PEG-b-PNIPA were dissolved in ultrapure water to prepare 1 wt% sample solutions. The sample solutions were placed in a 1 cm path length quartz glass cell and maintained at 20 °C in a water-cooled Peltier unit. The temperature was increased from 20 °C to 50 °C, and the transmittance changes were observed (heating rate of 0.5 °C/min, observation wavelength of 500 nm). Data were collected at intervals of 0.2 °C.

2.12. Dynamic Light Scattering (DLS) Measurement

The DLS measurements were conducted using a Zetasizer Nano ZS from Malvern, Malvern, UK (He-Ne ser, beam wavelength 633 nm). The measurements were performed at a scattering angle of 173° and at 25 °C, with 12 measurements over a 10 s period.

2.12.1. DLS Measurement of End- N_3 4-Arm Star-Shaped PEG-b-PNIPA in Various Solvents

End- N_3 4-arm star-shaped PEG-b-PNIPA was dissolved at 1 wt% in 1.5 mL of MeOH, DMF, THF, and acetonitrile to prepare four different solutions. After ultrasonic treatment for 30 min, the solutions were left to stand overnight. Each polymer solution was filtered through a 0.45 μm membrane filter (Millex-LCR 13 mm), and

1–1.5 mL was injected into the measurement cell. DLS measurements were performed, and the scattering intensity was measured 12 times.

2.12.2. DLS Measurement of End-N₃ 4-Arm Star-Shaped PEG-b-PNIPA

Various amounts of end-N₃ 4-arm star-shaped PEG-b-PNIPA were weighed and dissolved in 1.5 mL of acetonitrile to prepare solutions with volume fractions $\Phi = 1.6 \times 10^{-3}$ to 0.200. After 30 min of ultrasonic treatment, the solutions were left to stand overnight. The obtained polymer solutions were filtered through a membrane filter (Millex-LCR 13 mm, pore size 0.45 μm), and 1–1.5 mL was injected into the measurement cell. DLS measurements were conducted, and the scattering intensity of each solution was measured 12 times. Additionally, for end-N₃ 4-arm star-shaped PNIPA, solutions of varying concentrations were prepared using the same method, and the scattering intensity was evaluated through DLS measurements.

2.13. Small-Angle X-ray Scattering (SAXS) Measurement

SAXS measurements were conducted to analyze the network structure of PEG-b-PNIPA gels at the BL05XU beamline in SPring-8 (Hyogo, Japan). The prepared gels, swollen in either water or acetonitrile, were irradiated with X-rays of 0.1 nm wavelength. The scattered X-rays were detected using a PILATUS3S 1M detector (DECTRIS Ltd., Baden, Switzerland) positioned at a sample-to-detector distance of 3.9 m.

2.14. Gel Swelling Degree Test

2.14.1. Equilibrium Swelling Degree in Water and Acetonitrile

PEG-b-PNIPA gels synthesized at three different concentrations ($\Phi = 0.08, 0.12, 0.16$) were prepared inside capillaries with an inner diameter of 1.1 mm. The gels were soaked in MeOH for several days to remove unreacted substances, then equilibrated in acetonitrile and pure water. The gel diameter, D , was measured using a digital microscope (VHX-X1, Keyence, Osaka, Japan), and the swelling degree was calculated using the following formula:

$$\text{Swelling Degree} = D/D_0 \quad (1)$$

, where D_0 is the initial diameter of 1.1 mm, and D is the diameter after solvent exchange.

2.14.2. Temperature Dependence of Equilibrium Swelling Degree

PNIPA gel (initial concentration $\Phi = 0.1$) and PEG-b-PNIPA gel (initial concentration $\Phi = 0.08$) were synthesized as cylindrical gels inside capillaries with an inner diameter of 1.1 mm. After soaking the gels in MeOH for several days and further soaking them in pure water for several days, they were immersed in ultrapure water in a jacketed beaker connected to a circulation temperature control unit (Lauda RE104). The temperature was gradually increased from 20 °C, and the appearance and diameter of the equilibrated gels were observed using a digital microscope (VHX-X1) approximately every day. The diameter was measured three times, and the average value was used.

3. Results and Discussion

3.1. Synthesis of Initiator

The ¹H NMR measurement results of the obtained product are shown in Figure S1. The integral ratios of each peak were found to be a:b:c:d = 3:1:1:52, confirming the successful synthesis of the target initiator.

3.2. Synthesis of End-Cl 4-Arm Star-Shaped PEG-b-PNIPA

To monitor the progress of the reaction, ¹H NMR spectra were measured for samples taken at various time points, and the conversion from monomer to polymer was calculated. The proton signal for the vinyl group of NIPA (2H, 6.2 ppm) and the aldehyde proton of the solvent DMF (1H, 8.0 ppm) were observed at distinct positions. As the reaction proceeded, the intensity of the signal from the vinyl proton of NIPA decreased (Figure S2). The integral ratio of the peak from the vinyl proton of NIPA (I_{NIPAt}) was determined with the aldehyde proton signal of DMF as the reference. Similarly, the integral ratio of the vinyl proton of NIPA in the monomer solution was calculated as I_{NIPAO} . The monomer conversion rate for each reaction time was calculated using the following equation:

$$\text{conversion}(\%) = \left(1 - \frac{I_{\text{NIPAt}}}{I_{\text{NIPAO}}}\right) \times 100 \quad (2)$$

The monomer conversion rates as a function of reaction time are shown in Figure 3a. The conversion rate exceeded 90% after 10 min and reached 99% after 120 min, indicating that the reaction was very fast and efficient.

Next, SEC results and the molecular weight and molecular weight distribution relative to the reaction rate are shown in Figure 3b,c. A narrow molecular weight distribution and polymers with molecular weights corresponding to the input ratio were obtained.

Furthermore, the obtained sample was dissolved in acetone- d_6 , and ^1H NMR measurements were performed. The results are shown in Figure 3d. A signal (g) from the methine proton adjacent to the end-Cl of the 4-arm star-shaped PEG-b-PNIPA was observed around 4.8 ppm.

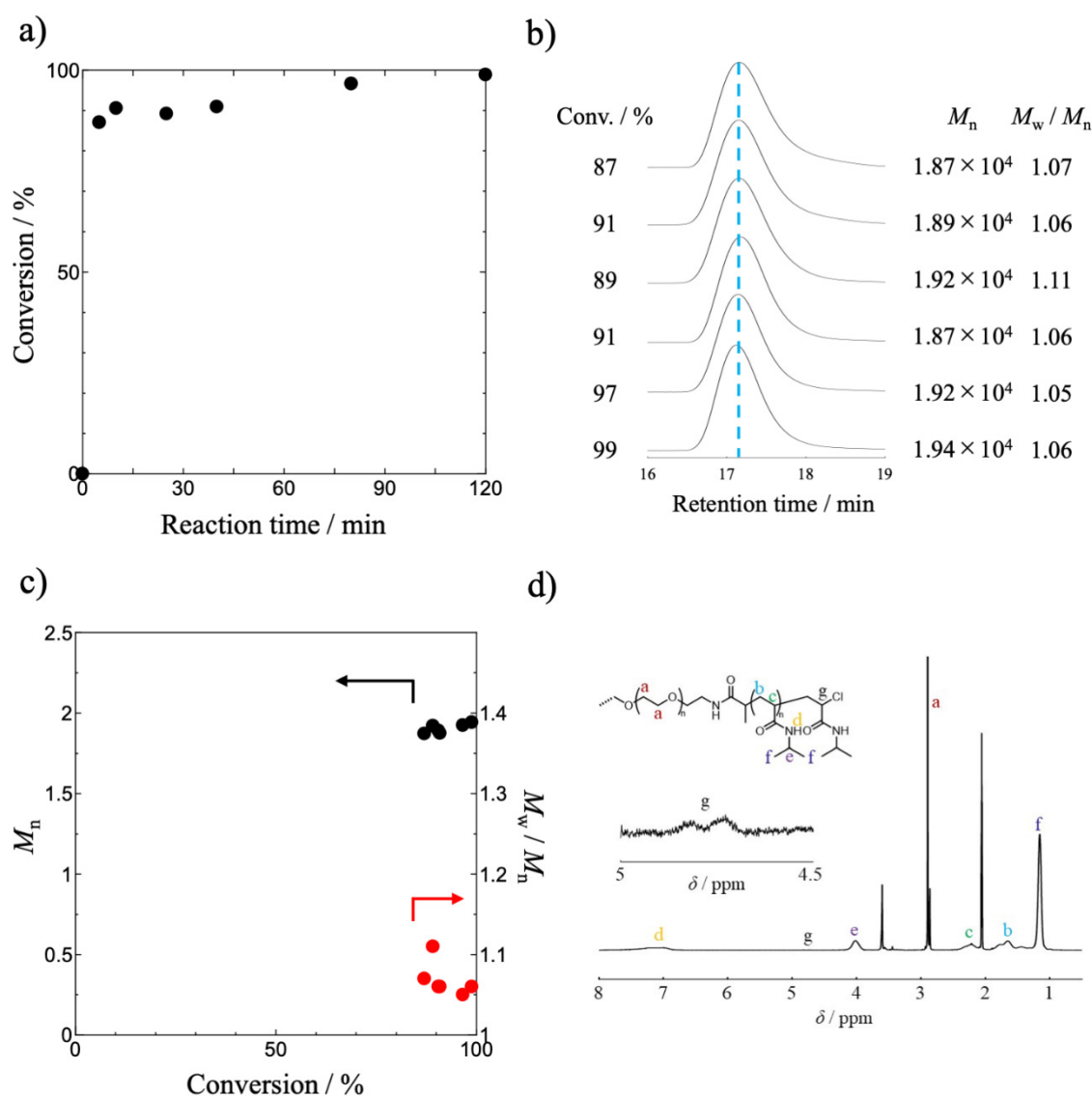


Figure 3. (a) Monomer conversion with polymerization time during SET-LRP of NIPA measured by ^1H NMR, (b) Evolution of SEC traces with polymerization time during SET-LRP of NIPA, (c) Number average molecular weight, M_n , and polydispersity index (M_w/M_n) vs. conversion plots, (d) ^1H NMR spectrum of end-Cl 4-arm star-shaped PEG-b-PNIPA.

3.3. Synthesis of End- N_3 4-Arm Star-Shaped PEG-b-PNIPA

The ^1H NMR measurement results for end- N_3 4-arm star-shaped PEG-b-PNIPA are shown in Figure 4a. The signal (g) from the methine proton adjacent to the end-Cl, observed in end-Cl 4-arm star-shaped PEG-b-PNIPA, was confirmed to have disappeared. However, the expected signal (h) from the methine proton adjacent to the end- N_3 was not observed in the ^1H NMR spectrum.

The FT-IR measurement results of end-Cl 4-arm star-shaped PEG-b-PNIPA and end-N₃ 4-arm star-shaped PEG-b-PNIPA are shown in Figure 4b. After azidation, a peak at 2110 cm⁻¹ was observed, which was not present before the azidation [17]. This peak, characteristic of the stretching vibration of the end-N₃ group, confirmed that azidation had occurred. From these results, it was confirmed that the end-Cl was successfully replaced with N₃ using this experimental method.

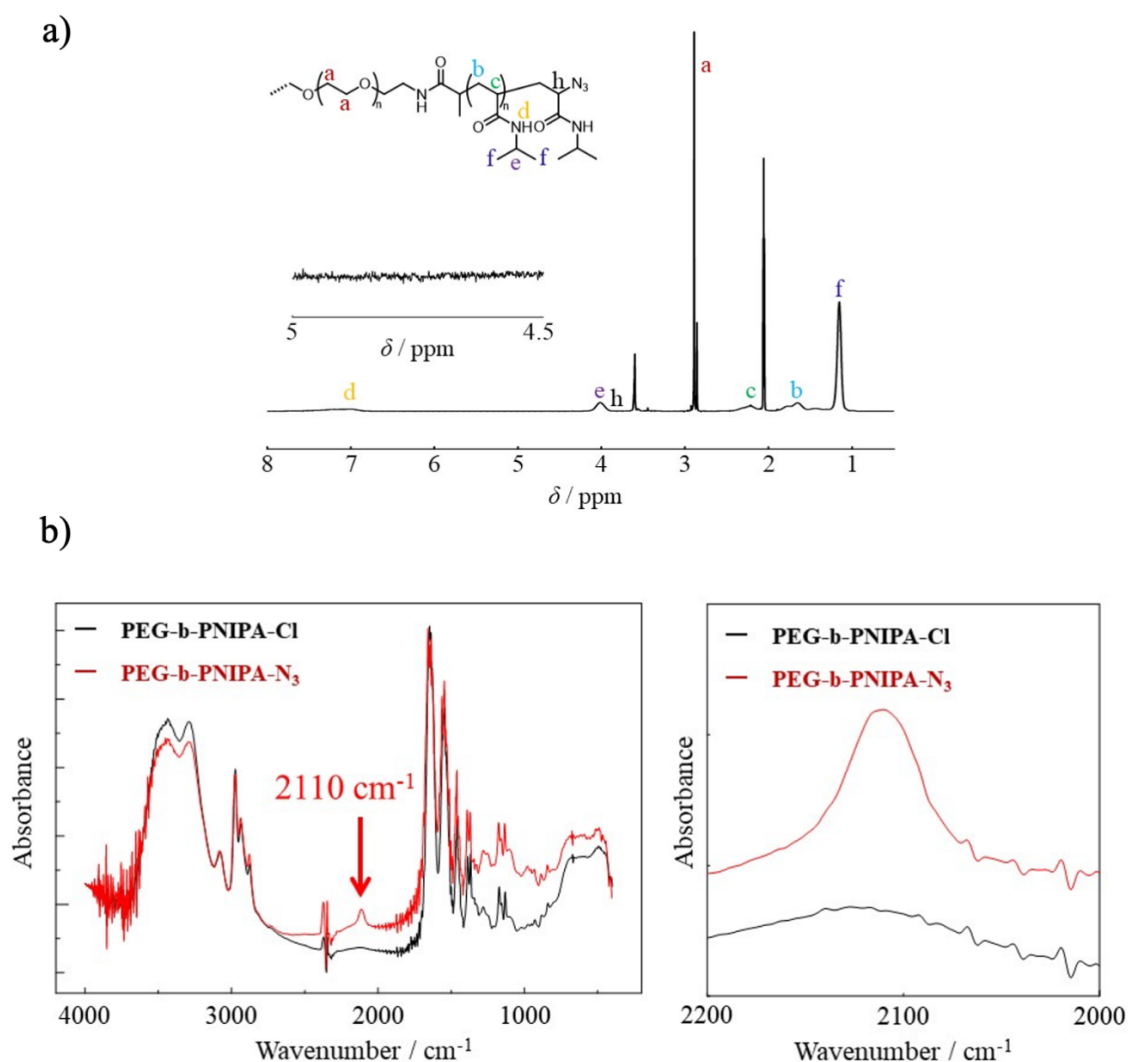


Figure 4. (a) ¹H NMR spectrum of end-N₃ 4-arm star-shaped PEG-b-PNIPA, (b) FT-IR spectra obtained for 4-arm star-shaped PEG-b-PNIPA (black) before azidation (red) after azidation.

3.4. Azidation Reaction Rate of End-N₃ 4-Arm Star-Shaped PEG-b-PNIPA

The terminal azidation rate could not be directly evaluated from the results in Section 3.3. Therefore, DBCO-amine was introduced into the azidated end-4-arm star-shaped PEG-b-PNIPA through a click reaction, and the azidation reaction rate was determined by measuring the ¹H NMR of the resulting product. The results of ¹H NMR measurements and FT-IR are shown in Figure 5. A peak (g) corresponding to the proton of the benzene ring in DBCO-amine was observed between 7–8 ppm (Figure 5a). Thus, the ¹H NMR spectra before and after the click reaction, focusing on the 4–8 ppm range, are shown in Figure 5b,c. Before the click reaction, the integral ratio of peaks d and e in the PNIPA repeat unit was 1.0453:1. After the click reaction, the integral ratio of d and e, along with the peak g from the benzene ring of DBCO, was 1.1907:1. These results yield a g:e ratio of 0.1454, or e/g = 6.88. Since one arm of the 4-arm star-shaped polymer was synthesized to be 50 units long, the theoretical value for e/g is 6.25. Therefore, it was confirmed that more than 91% of the terminal azide groups were introduced. Furthermore, in FT-IR, it was confirmed that the peak from the terminal N₃ group disappeared after the reaction with DBCO-amine (Figure 5d).

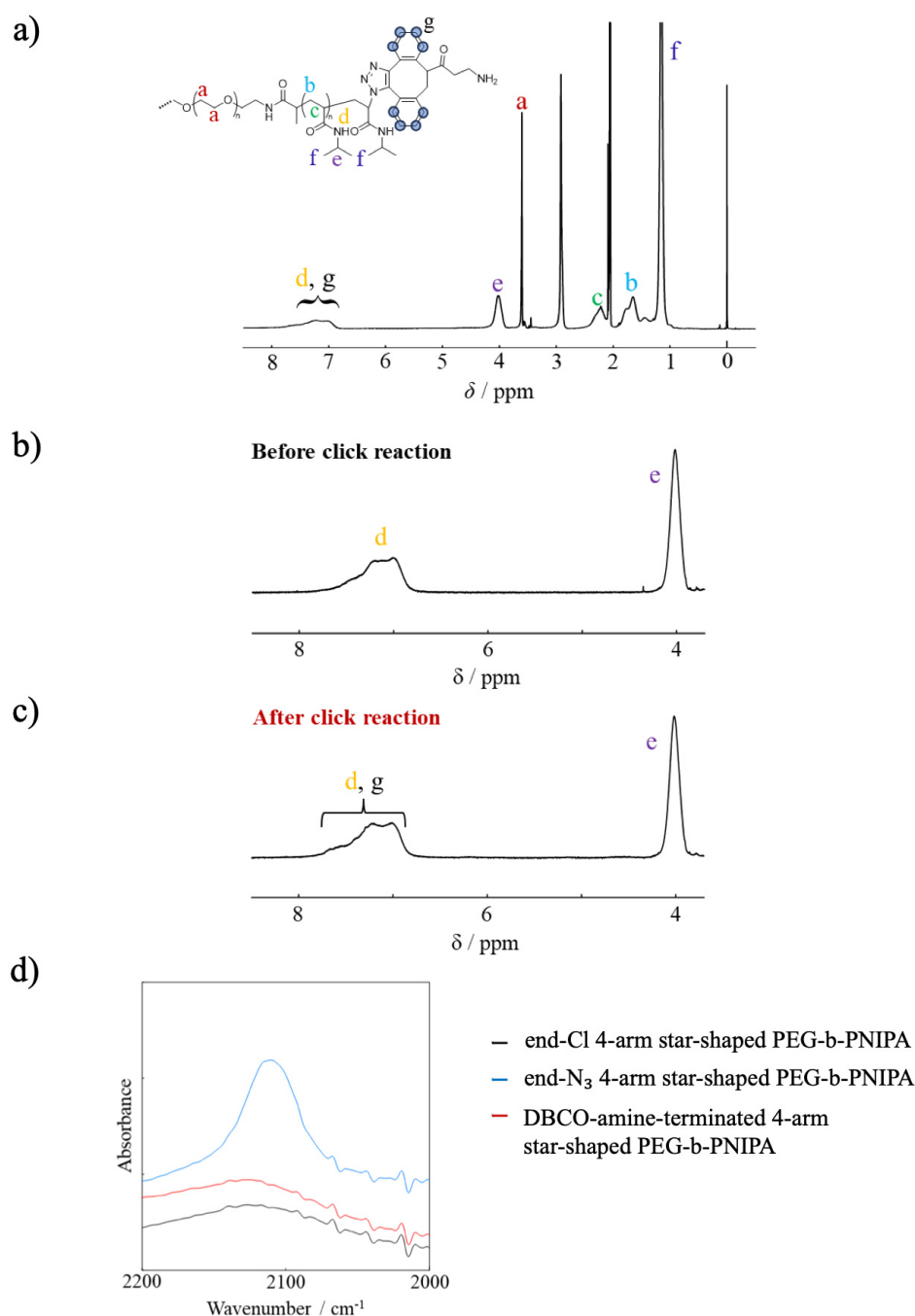


Figure 5. (a) ^1H NMR spectra of DBCO-amine-terminated 4-arm star-shaped PEG-b-PNIPA, (b) ^1H NMR of end- N_3 4-arm star-shaped PEG-b-PNIPA before reaction with DBCO-amine, (c) ^1H NMR of end- N_3 4-arm star-shaped PEG-b-PNIPA after reaction with DBCO-amine, (d) FT-IR spectra obtained for end-Cl 4-arm star-shaped PEG-b-PNIPA (black), end- N_3 4-arm star-shaped PEG-b-PNIPA (blue), DBCO-amine-terminated 4-arm star-shaped PEG-b-PNIPA (red).

3.5. UV-Vis Transmittance Measurement

Figure 6 shows the UV-Vis transmittance of aqueous solutions of terminal Cl 4-arm star-shaped PNIPA and terminal Cl, N_3 4-arm star-shaped PEG-b-PNIPA as a function of temperature. All polymers formed colorless and transparent solutions at low temperatures, and underwent phase separation above a certain temperature, resulting in turbid solutions. The temperatures at which the solutions of each polymer became turbid, determined from the transmittance data, are summarized in Table 1. The temperature at which the solution becomes turbid (transition temperature)—defined as the temperature where the transmittance drops below 99%—correlates with the LCST. The star-shaped polymer consisting solely of PNIPA with terminal Cl groups and without PEG segments turned turbid at 33.5 °C. This behavior is nearly identical to that of conventional linear PNIPA. In contrast, the PEG-b-PNIPA bearing Cl terminal groups and incorporating PEG segments became turbid at 37.0 °C, which is 3.5 °C

higher. This shift is attributed to the increased hydrophilicity of the polymer due to the presence of the hydrophilic PEG chains. These results also suggest that the nature of the terminal groups affects LCST behavior.

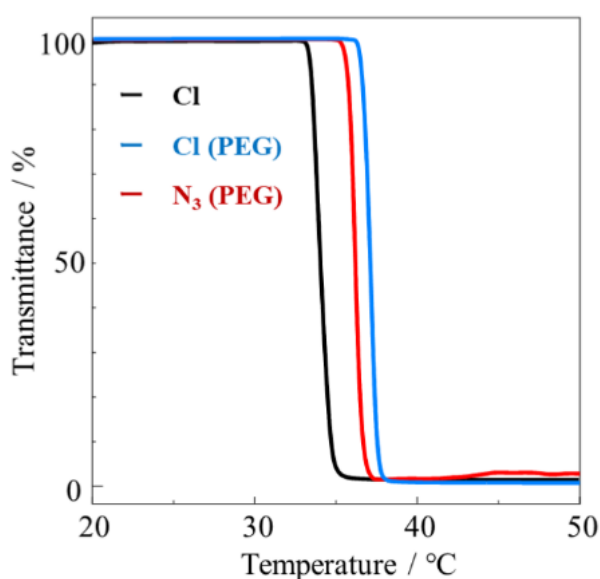


Figure 6. Dependence of transmittance on temperature of end-Cl 4-arm star-shaped PNIPA, end-Cl 4-arm star-shaped PEG-b-PNIPA, and end-N₃ 4-arm star-shaped PEG-b-PNIPA in pure water.

Table 1. Transition temperature of tetra branched PNIPA and PEG-b-PNIPA.

Termination	Transition Temperature/°C
Cl	33.5
Cl (PEG)	37.0
N ₃ (PEG)	36.0

3.6. DLS Measurement of End-N₃ 4-Arm Star-Shaped PEG-b-PNIPA

In order to synthesize a gel with an ordered network structure, it is essential to use a solvent with high affinity for the polymer, as well as to densely pack the polymer chains in the solution and fill the space uniformly. Therefore, we first selected an appropriate good solvent for end-N₃ 4-arm star-shaped PEG-b-PNIPA. The DLS results of 1 wt% N₃ 4-arm star-shaped PEG-b-PNIPA solutions dissolved in various solvents (Figure S3) were compared, and acetonitrile was selected as it showed the best dispersion properties.

Next, different volume fractions of end-N₃ 4-arm star-shaped PEG-b-PNIPA were dissolved in acetonitrile, and the scattering intensity was measured to estimate the overlap volume fraction of the polymer. Since the autocorrelation functions of all polymer solutions prepared in this study exhibited sigmoid behavior, it was confirmed that no significant aggregation of the polymer occurred in these solutions (Figure S4).

The volume of the polymer in the solution (V_p) can be calculated using its molar concentration (c) with the following equation:

$$V_p = \frac{cV_sM_w}{d} \quad (3)$$

Here, V_s is the volume of the solvent (acetonitrile), M_w is the molecular weight of the polymer (the molecular weight of the end-N₃ 4-arm star-shaped PEG-b-PNIPA is $M_w = 2.0 \times 10^4 \text{ g mol}^{-1}$), and d is the density of the polymer ($1.34 \times 10^3 \text{ g L}^{-1}$). Therefore, the volume fraction (Φ) of the polymer chain can be calculated using the following equation:

$$\Phi = \frac{V_p}{V_s + V_p} = \frac{\frac{cM_w}{d}}{1 + \frac{cM_w}{d}} \quad (4)$$

The results of plotting the scattering intensity against the volume fraction ($\Phi = 1.6 \times 10^{-3} \sim 0.200$) for acetonitrile solutions of end-N₃ 4-arm star-shaped PEG-b-PNIPA at different concentrations, obtained by DLS measurement, are shown in Figure 7. The scattering intensity values used were corrected by subtracting the effect of the attenuator in the DLS apparatus. The region deviating from the theoretical scaling laws for dilute solutions

in a good solvent ($I \sim \Phi^1$) and semi-dilute solutions ($I \sim \Phi^{-1/4}$) was defined as the overlap region, which corresponds to the transition from the dilute region to the semi-dilute region of the polymer [21,22]. The boundary between the overlap region and the semi-dilute region, $\Phi = 0.05$, was defined as the overlap volume fraction (c^*).

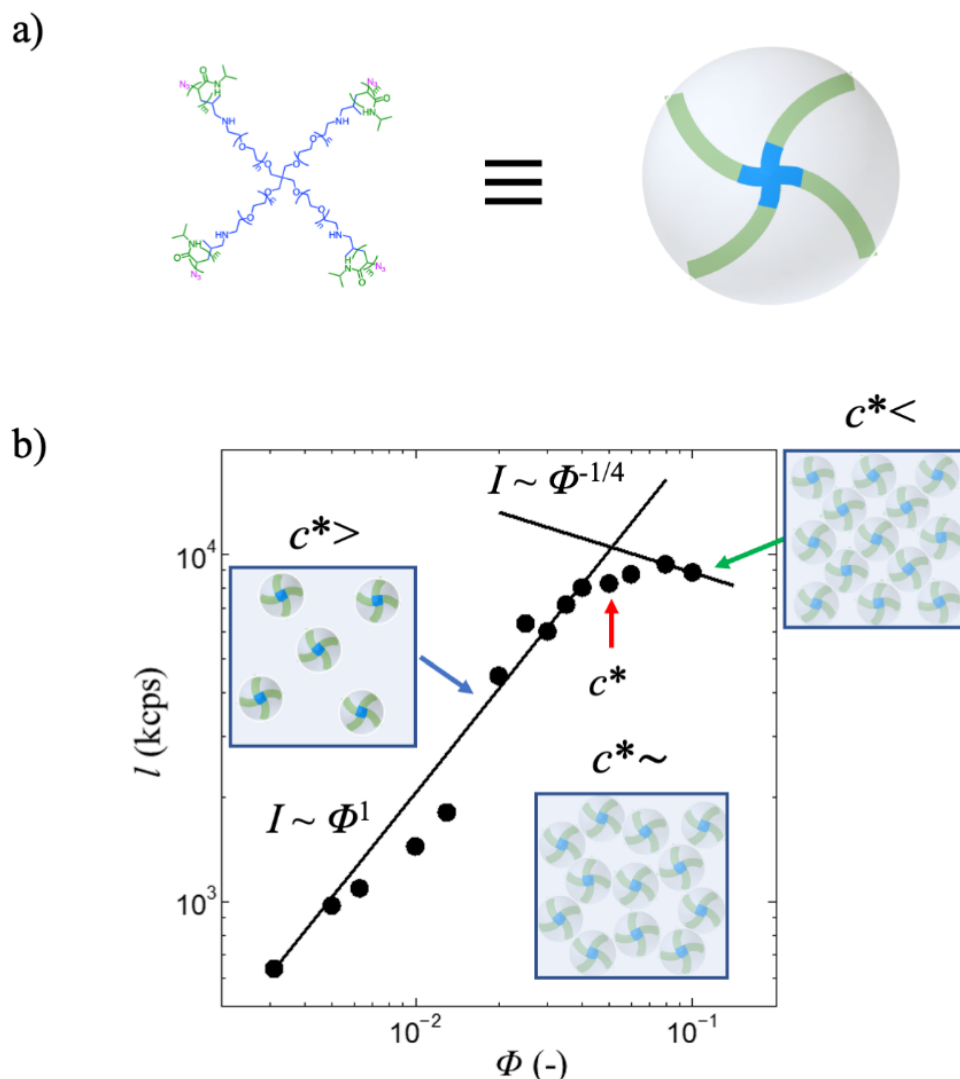


Figure 7. (a) Schematic of end-N₃ 4-arm star-shaped PEG-b-PNIPA, (b) Scattering intensity (I) of end-N₃ 4-arm star-shaped PEG-b-PNIPA in acetonitrile for various polymer volume fractions.

Similarly, the value of c^* for end-N₃ 4-arm star-shaped PNIPA was estimated using the same method. The molecular weight of end-N₃ 4-arm star-shaped PNIPA is $M_w = 2.9 \times 10^4 \text{ g mol}^{-1}$, and the polymer density is $1.4 \times 10^3 \text{ g L}^{-1}$. From the results shown in Figure S5, $\Phi = 0.07$ was taken as the volume fraction of c^* .

3.7. Preparation of Gel via Huisgen Cycloaddition Reaction of End-N₃ 4-Arm Star-Shaped PEG-b-PNIPA or End-N₃ 4-Arm Star-Shaped PNIPA

The end-N₃ 4-arm star-shaped PEG-b-PNIPA acetonitrile solution, prepared at a semi-dilute concentration, was mixed with an appropriate amount of crosslinking agent (Figure 8a) and left at room temperature for 3 days. The right diagram in Figure 8a illustrates a polymer network with an ideal ordered structure, formed by the end-to-end crosslinking of four-arm star block copolymers with reactive termini, where each terminal group is connected to a different four-arm star block copolymer. The gelation process is shown in Figure 8b. In all four conditions with volume fractions $\Phi = 0.08, 0.095, 0.12$, and 0.16 , the click reaction shown in Figure 8c proceeded, and the gel was formed. For comparison, the PNIPA gel was prepared at a volume fraction $\Phi = 0.1$ ($1.4c^*$).

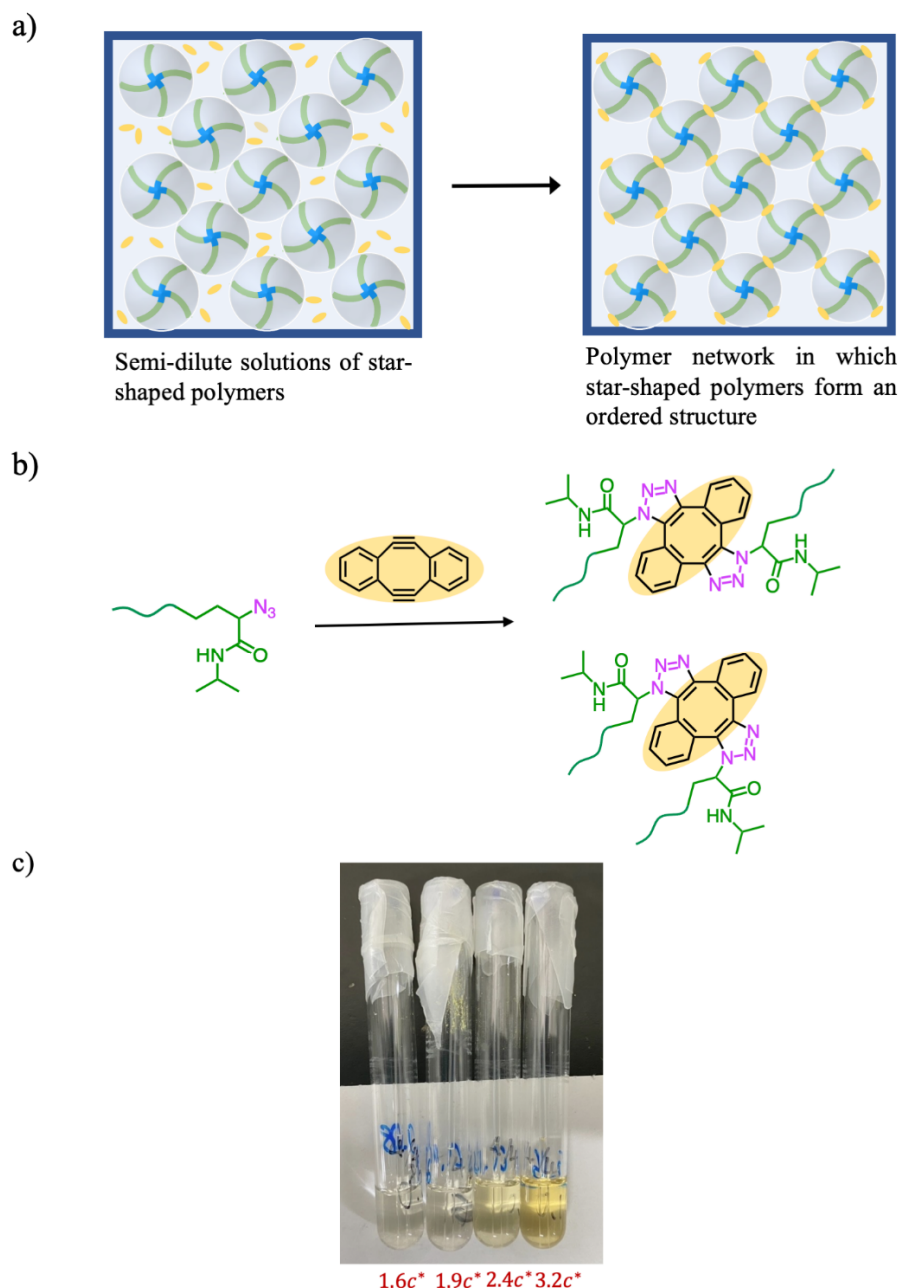


Figure 8. (a) Schematic of click reaction crosslinking of end-N₃ 4-arm star-shaped PEG-b-PNIPA under semi-dilute conditions, (b) Cross-linking of end-N₃ 4-arm star-shaped PEG-b-PNIPA by click reaction, (c) Photo of PEG-b-PNIPA gels.

3.8. Analysis of the Network Structure by SAXS

The polymer network structure of the PEG-b-PNIPA gels was analyzed using SAXS. Figure 9a shows the SAXS profiles of PEG-b-PNIPA gels with different prepared volume fractions, $\Phi = 0.08, 0.12$, and 0.16 , in pure water and acetonitrile. All the profiles are well described by the following equation [18,23,24]:

$$I(q) = \frac{I_{\text{OZ}}(0)}{1 + \xi_{\text{OZ}}^2 q^2} + Cq^{-d} + I_{\text{BKG}} \quad (5)$$

The first term is the Ornstein-Zernike (OZ) function with the correlation length ξ_{OZ} . The second term, Cq^{-d} , accounts for the upturn in the low- q region, where C is a constant and d is the power-law exponent. I_{BKG} represents the q -independent background. The solid lines in Figure 9a show the fitting results using Equation (5).

The increase in intensity at low- q may indicate a two-phase structure that has a sharp interface, consistent with Porod's law ($\propto q^{-4}$). However, for the $\Phi = 0.08$ in both water and acetonitrile, this contribution is negligible. At higher volume fractions ($\Phi = 0.12$ and 0.16), the power law exponent d ranges from 2.3 to 3.4, suggesting the presence of a fractal structure. The low- q upturn may be therefore attributed to aggregated formation.

Figure 9b shows the Φ -dependence of ξ_{OZ} . At all volume fractions, ξ_{OZ} is larger in water than in acetonitrile, reflecting the higher degree of swelling in water. In both solvents, ξ_{OZ} decreases with increasing Φ , indicating that gels with higher prepared volume fractions possess more densely crosslinked networks.

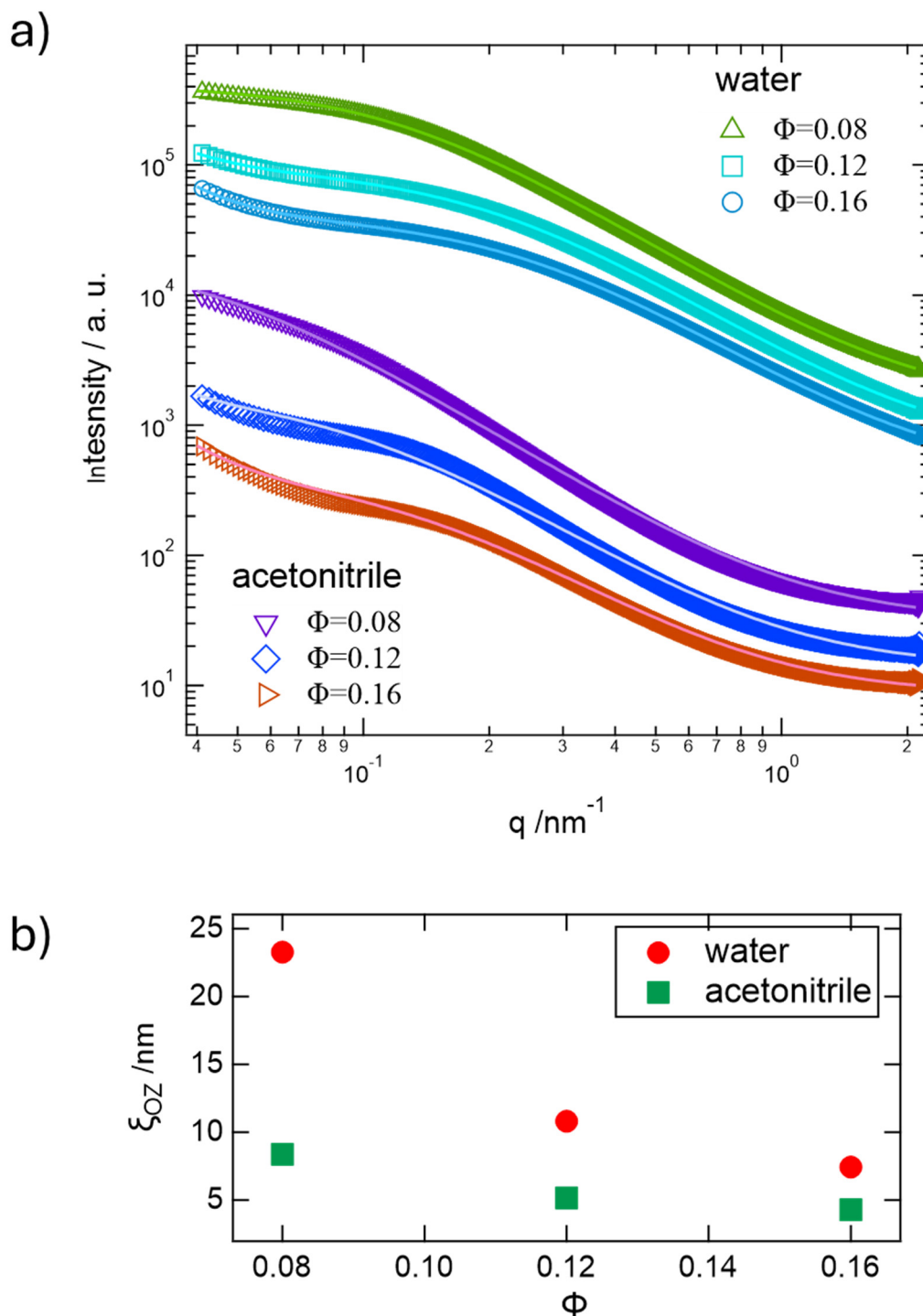


Figure 9. (a) SAXS profiles of PEG-b-PNIPAM gels with different prepared volume fractions, $\Phi = 0.08$, 0.12 , and 0.16 , in pure water and acetonitrile. (b) Φ -dependence of the correlation length ξ_{OZ} .

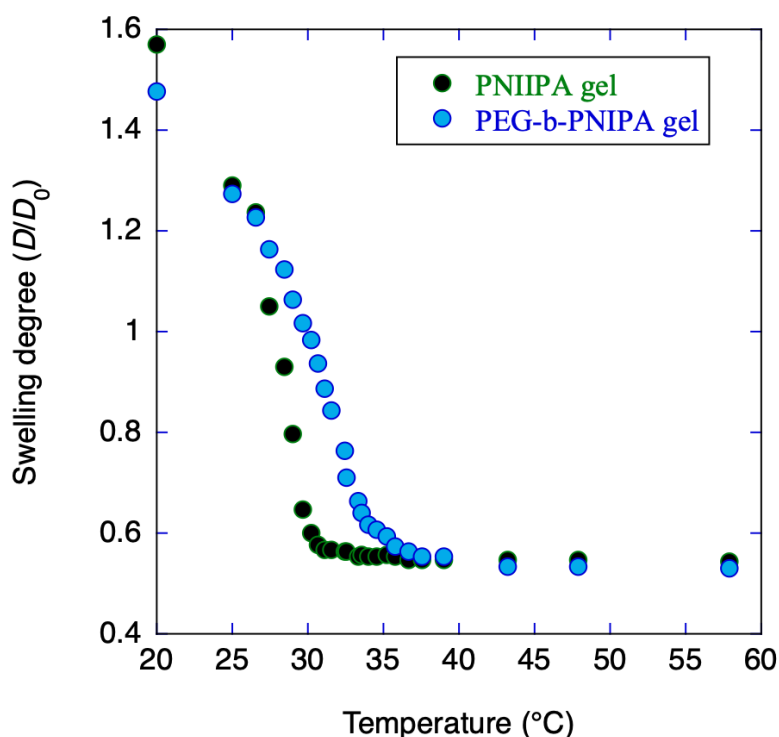
3.9. Equilibrium Swelling Degree Measurement

3.9.1. Measurement and Comparison of Transition Temperature

The equilibrium swelling degree of the PNIPA gel (prepared at $\Phi = 0.1$) and PEG-b-PNIPA gel (prepared at $\Phi = 0.08$) was measured during the heating process from 20°C to 60°C , and the swelling curves are shown in

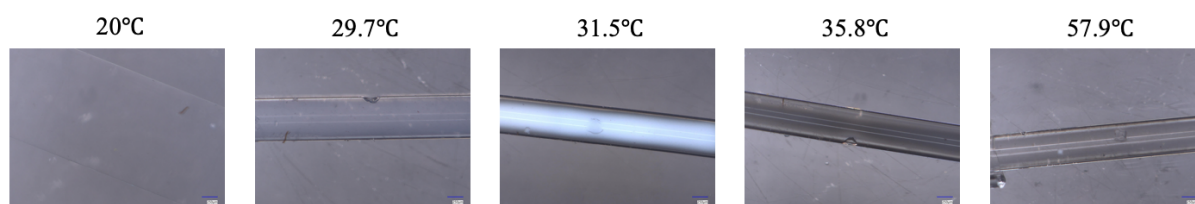
Figure 10. From the derivative curve of these results, the temperature where the absolute value of the slope is maximum was defined as the transition temperature.

a)



b)

PNIPA gel ($\phi = 0.1$)



PEG-b-PNIPA gel ($\phi = 0.08$)

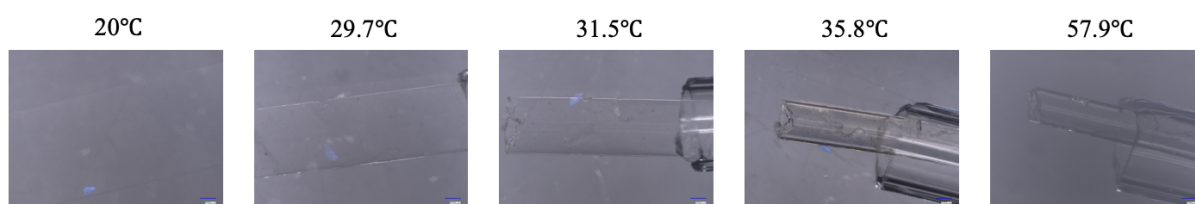


Figure 10. (a) Swelling curves of PNIPA gel and PEG-b-PNIPA gel, (b) Microscopic photographs of PNIPA gel and PEG-b-PNIPA gel observed when set at a certain temperature.

For the PNIPA gel, the transition temperature was 27 °C. Generally, the transition temperature of PNIPA gels prepared by free radical polymerization with crosslinkers like BIS is around 32.0 °C. Comparing the 4-arm star-shaped PNIPA gel crosslinked with DIBOD and the conventional PNIPA gel, a decrease of about 5 °C was observed. This decrease can be attributed to the fact that DIBOD is a hydrophobic compound with large aromatic rings. The introduction of DIBOD likely altered the hydrophilic/hydrophobic balance of the network, shifting the transition temperature to a lower temperature.

On the other hand, the PEG-b-PNIPA gel showed a transition temperature of 32.5 °C. Compared to the 4-arm star-shaped PNIPA gel, the transition temperature was 5.5 °C higher. This difference is attributed to the presence of the hydrophilic PEG. In the PEG-b-PNIPA gel, the introduction of PEG increased the overall

hydrophilicity of the network, causing the transition temperature to shift to a higher temperature. This result reflects the LCST observed in the solution, as shown in Figure 6 and Table 1.

3.9.2. Optical Changes of the Gel Near the Transition Temperature

Significant differences were observed in the state changes of the gel during the temperature increase near the transition temperature.

In the PNIPA gel, as the temperature increased, the entire gel contracted and became cloudy (Figure 10b). This behavior is similar to that observed in conventional PNIPA gels prepared by free radical polymerization, where an unstable phase is formed upon heating, and phase separation occurs within the gel. The polymer network density becomes heterogeneous, forming regions of low and high density. When the size of these regions becomes comparable to the wavelength of light, light scattering occurs, causing cloudiness. In such a state, it takes a long time to reach thermodynamic equilibrium, and the optically cloudy state tends to persist [25].

In contrast, the PEG-b-PNIPA gel maintained its transparency during the temperature rise near the transition temperature, with no cloudiness observed. This is because the hydrophilic PEG is uniformly distributed within the network, suppressing phase separation due to the temperature-responsive behavior of PNIPA and its interaction with the solvent. As a result, even though volume shrinkage occurred due to temperature changes, the gel retained its transparency and quickly reached the equilibrium state. In other words, with these properties, the shrinkage behavior of the gel can be explained by the cooperative diffusion equation, and the decrease in shrinkage rate due to phase separation, as observed in conventional PNIPA gels, will no longer occur.

4. Conclusions

In this study, a temperature-responsive polymer network was successfully synthesized by using a 4-arm star-shaped polyethylene glycol (PEG) derivative as an initiator to polymerize *N*-isopropylacrylamide (NIPA) as the secondary acrylamide. The resulting star-shaped block copolymer served as a key building block for the construction of the polymer network.

Through detailed analysis of the polymerization process, it was confirmed that the 4-arm star-shaped PEG-b-PNIPA structure was synthesized under high control. The structure was clearly verified by SEC and ¹H NMR measurements. Furthermore, the terminal group conversion efficiency using click chemistry was evaluated, and over 91% azidation was confirmed by ¹H NMR and FT-IR spectroscopy. SAXS measurements indicate that the PEG-b-PNIPA gels have a more densely cross-linked networks. Additionally, UV-Vis transmittance measurements showed that the introduction of PEG increased the LCST of the gel, enhancing its hydrophilicity and transparency.

The obtained gel exhibited unique characteristics of volume shrinkage while maintaining optical transparency upon heating. This behavior is thought to result from the effective suppression of phase separation during the shrinkage process due to the regular introduction of PEG within the polymer network. The maintenance of transparency during shrinkage overcomes the main limitation of conventional PNIPA-based gels and expands the applicability to optical sensors, actuators, and biomedical devices.

These results suggest the promising potential of this polymer network design for the development of advanced smart materials. Future research will focus on optimizing the mechanical properties of the gel and exploring its potential applications in stimulus-responsive devices. By precisely adjusting the polymer composition and crosslinking strategy, the development of next-generation materials with suitable responsiveness and durability for practical environments is aimed for.

Supplementary Materials: The following supporting information can be downloaded at: <https://media.sciltp.com/articles/others/2507101000153971/MI-957-SI.pdf>, Figure S1: ¹H NMR spectrum of initiator prepared from 4-Arm PEG-Amine; Figure S2: Time change of ¹H NMR spectra of the reaction solution for preparation of end-Cl 4-arm star-shaped PEG-b-PNIPA; Figure S3: Correlation coefficient of end-N₃ 4-arm star-shaped PEG-b-PNIPA in various solvents (MeOH, DMF, THF, acetonitrile); Figure S4: Correlation coefficients observed from solutions of end-N₃ 4-arm star-shaped PEG-b-PNIPA dissolved in various concentrations of acetonitrile; Figure S5: Scattering intensity (I) of end-N₃ 4-arm star-shaped PEG-b-PNIPA in Acetonitrile for various polymer volume fractions.

Author Contributions: K.K.: Performed all experiments. Writing the original draft, conducting investigations, and generating graphs. T.H.: Performed SAXS measurements. Writing the original draft, conducting investigations, and generating graphs. Y.T.: Managing the project, acquiring funding, supervising, writing the original draft, reviewing, revising, and editing. All authors have read and agreed to the published version of the manuscript.

Funding: This work is supported by Toshiaki Ogasawara Memorial Foundation.

Data Availability Statement: Raw data will be made available upon reasonable request.

Acknowledgments: *N*-isopropylacrylamide (NIPA) was kindly obtained from KJ Chemicals. Tris(2-dimethylaminoethyl)amine (Me₆TREN) was provided by Mitsubishi Chemical.

Conflicts of Interest: The authors declare no conflict of interest.

References

- Seuring, J.; Agarwal, S. Polymers with Upper Critical Solution Temperature in Aqueous Solution: Unexpected Properties from Known Building Blocks. *ACS Macro Lett.* **2013**, *2*, 597–600. <https://doi.org/10.1021/mz400227y>.
- Zhang, Q.L.; Hoogenboom, R. Polymers with upper critical solution temperature behavior in alcohol/water solvent mixtures. *Prog. Polym. Sci.* **2015**, *48*, 122–142. <https://doi.org/10.1016/j.progpolymsci.2015.02.003>.
- Cook, M.T.; Haddow, P.; Kirton, S.B.; McAuley, W.J. Polymers Exhibiting Lower Critical Solution Temperatures as a Route to Thermoreversible Gelators for Healthcare. *Adv. Funct. Mater.* **2021**, *31*, 2008123. <https://doi.org/10.1002/adfm.202008123>.
- Zhang, X.; Zhang, P.P.; Lu, M.; Qi, D.M.; Müller-Buschbaum, P.; Zhong, Q. Synergistic Stain Removal Achieved by Controlling the Fractions of Light and Thermo Responsive Components in the Dual-Responsive Copolymer Immobilized on Cotton Fabrics by Cross-Linker. *ACS Appl. Mater. Interfaces* **2021**, *13*, 27372–27381. <https://doi.org/10.1021/acsami.1c03290>.
- Ueki, T.; Watanabe, M. Polymers in Ionic Liquids: Dawn of Neoteric Solvents and Innovative Materials. *Bull. Chem. Soc. Jpn.* **2012**, *85*, 33–50. <https://doi.org/10.1246/bcsj.20110225>.
- Das, A.; Babu, A.; Chakraborty, S.; Van Guyse, J.F.R.; Hoogenboom, R.; Maji, S. Poly(-isopropylacrylamide) and Its Copolymers: A Review on Recent Advances in the Areas of Sensing and Biosensing. *Adv. Funct. Mater.* **2024**, *34*, 2402432. <https://doi.org/10.1002/adfm.202402432>.
- Jiang, L.; Qin, D.N.; Zhang, C.F.; Cui, J.B.; Xu, X.Y.; Hu, R.; Zhang, P.; Hu, L. Poly(-isopropylacrylamide) Microgel-Based Sensor for Clinical-Level X-ray Dose Measurements. *ACS Appl. Polym. Mater.* **2023**, *5*, 10073–10080. <https://doi.org/10.1021/acsapm.3c01924>.
- Bergbreiter, D.E.; Case, B.L.; Liu, Y.S.; Caraway, J.W. Poly(N-isopropylacrylamide) soluble polymer supports in catalysis and synthesis. *Macromolecules* **1998**, *31*, 6053–6062. <https://doi.org/10.1021/ma980836a>.
- Liu, M.; Song, X.; Wen, Y.T.; Zhu, J.L.; Li, J. Injectable Thermoresponsive Hydrogel Formed by Alginate—Poly(-isopropylacrylamide) That Releases Doxorubicin-Encapsulated Micelles as a Smart Drug Delivery System. *ACS Appl. Mater. Interfaces* **2017**, *9*, 35673–35682. <https://doi.org/10.1021/acsami.7b12849>.
- Kim, T.H.; Choi, J.G.; Byun, J.Y.; Jang, Y.; Kim, S.M.; Spinks, G.M.; Kim, S.J. Biomimetic Thermal-sensitive Multi-transform Actuator. *Sci. Rep.* **2019**, *9*, 7905. <https://doi.org/10.1038/s41598-019-44394-x>.
- Maeda, S.; Hara, Y.; Sakai, T.; Yoshida, R.; Hashimoto, S. Self-walking gel. *Adv. Mater.* **2007**, *19*, 3480–3484. <https://doi.org/10.1002/adma.200700625>.
- Shibayama, M. Physics of polymer gels: Toyochi Tanaka and after. *Soft Matter* **2025**, *21*, 1995–2009. <https://doi.org/10.1039/d4sm01418a>.
- Takeoka, Y.; Watanabe, M. Polymer gels that memorize structures of mesoscopically sized templates. Dynamic and optical nature of periodic ordered mesoporous chemical gels. *Langmuir* **2002**, *18*, 5977–5980. <https://doi.org/10.1021/la020133t>.
- Yoshida, R.; Uchida, K.; Kaneko, Y.; Sakai, K.; Kikuchi, A.; Sakurai, Y.; Okano, T. Comb-Type Grafted Hydrogels with Rapid De-Swelling Response to Temperature-Changes. *Nature* **1995**, *374*, 240–242. <https://doi.org/10.1038/374240a0>.
- Yasumoto, A.; Gotoh, H.; Gotoh, Y.; Bin Imran, A.; Hara, M.; Seki, T.; Sakai, Y.; Ito, K.; Takeoka, Y. Highly Responsive Hydrogel Prepared Using Poly(N-isopropylacrylamide)-Grafted Polyrotaxane as a Building Block Designed by Reversible Deactivation Radical Polymerization and Click Chemistry. *Macromolecules* **2017**, *50*, 364–374. <https://doi.org/10.1021/acs.macromol.6b01955>.
- Jochi, Y.; Seki, T.; Soejima, T.; Satoh, K.; Kamigaito, M.; Takeoka, Y. Spontaneous synthesis of a homogeneous thermoresponsive polymer network composed of polymers with a narrow molecular weight distribution. *NPG Asia Mater.* **2018**, *10*, 840–848. <https://doi.org/10.1038/s41427-018-0074-x>.
- Okaya, Y.; Jochi, Y.; Seki, T.; Satoh, K.; Kamigaito, M.; Hoshino, T.; Nakatani, T.; Fujinami, S.; Takata, M.; Takeoka, Y. Precise Synthesis of a Homogeneous Thermoresponsive Polymer Network Composed of Four-Branched Star Polymers with a Narrow Molecular Weight Distribution. *Macromolecules* **2020**, *53*, 374–386. <https://doi.org/10.1021/acs.macromol.9b01616>.
- Kwon, D.; Jochi, Y.; Okaya, Y.; Seki, T.; Satoh, K.; Kamigaito, M.; Hoshino, T.; Urayama, K.; Takeoka, Y. Nonturbid Fast Temperature-Responsive Hydrogels with Homogeneous Three-Dimensional Networks by Two Types of Star Polymer Synthesis Methods. *Macromolecules* **2021**, *54*, 5750–5764. <https://doi.org/10.1021/acs.macromol.1c00446>.
- Hiei, Y.; Ohshima, I.; Hara, M.; Seki, T.; Hoshino, T.; Takeoka, Y. Shrinking rates of polymer gels composed of star-shaped polymers of N-isopropylacrylamide and dimethylacrylamide copolymers: the effect of dimethylacrylamide on the

- crosslinking network. *Soft Matter*. **2022**, *18*, 5204–5217. <https://doi.org/10.1039/d2sm00402j>.
20. Gao, G.H.; Hara, M.; Seki, T.; Takeoka, Y. Synthesis of thermo-responsive polymer gels composed of star-shaped block copolymers by copper-catalyzed living radical polymerization and click reaction. *Sci. Technol. Adv. Mater.* **2024**, *25*, 2302795. <https://doi.org/10.1080/14686996.2024.2302795>.
21. Rubinstein, M.; Colby, R.H. *Polymer Physics*; Oxford University Press: Oxford, UK, 2003.
22. Li, X.; Nakagawa, S.; Tsuji, Y.; Watanabe, N.; Shibayama, M. Polymer gel with a flexible and highly ordered three-dimensional network synthesized via bond percolation. *Sci. Adv.* **2019**, *5*, eaax8647. <https://doi.org/10.1126/sciadv.aax8647>.
23. Shibayama, M. Spatial inhomogeneity and dynamic fluctuations of polymer gels. *Macromol. Chem. Phys.* **1998**, *199*, 1–30.
24. Matsunaga, T.; Sakai, T.; Akagi, Y.; Chung, U.; Shibayama, M. Structure Characterization of Tetra-PEG Gel by Small-Angle Neutron Scattering. *Macromolecules* **2009**, *42*, 1344–1351. <https://doi.org/10.1021/ma802280n>.
25. Tanaka, T.; Ishiwata, S.; Ishimoto, C. Critical Behavior of Density Fluctuations in Gels. *Phys. Rev. Lett.* **1977**, *38*, 771–774. <https://doi.org/10.1103/PhysRevLett.38.771>.